Nonlinear Dynamics and Systems Theory, **23** (5) (2023) 519–537

Performance Comparison of Sliding Mode Control and Sliding PID for Rescue ROV

T. Herlambang [1], A. Suryowinoto [2*], I. Kurniastuti [1], H. Nurhadi [3] and K. Oktafianto [4]

[1] *Department of Information Systems, Universitas Nahdlatul Ulama Surabaya, Indonesia.*
[2] *Electrical Engineering Department, Institut Teknologi Adhi Tama Surabaya, Indonesia.*
[3] *Department of Industrial Mechanical Engineering, Sepuluh Nopember Institute of Technology, Indonesia.*
[4] *Department of Mathematics, University of PGRI Ronggolawe, Indonesia.*

Received: July 31, 2022; Revised: October 17, 2023

Abstract: The underwater vehicle has been developed by many countries to be one kind of defense technology. This unmanned underwater vehicle is usually called the Remotely Operated Underwater Vehicle (ROV). The ROV is commonly used for underwater exploration and as a defense vehicle. The ROV can move by using six degrees of freedom (6-DOF) and requires a control system in order for the ROV to move as intended. In this paper, a controller was synthesized in the 6-DOF Evacuation ROV linear model with the Sliding Mode Control (SMC) and Sliding PID (SPID) methods. The contribution of the paper provides an analysis of numerical study and stability analysis by using the Lyapunov function for the performance of both control system methods. The focus of this paper is the comparison between the performance of SMC and SPID on the AUV linear model, of which SPID is a combination of SMC and PID. The simulation results show that the SMC and SPID methods have a good stability and small error of about 0.1% - 4%. Further, the results show that the SPID method is more stable than SMC.

Keywords: *remotely operated underwater vehicle; sliding mode control; sliding proportional integral derivative; linear model; Lyapunov function.*

Mathematics Subject Classification (2010): 93C10, 93D05.

* Corresponding author: mailto:andysuryo@itats.ac.id

1 Introduction

Underwater robots are widely developed by many countries as one of their defense technologies. The underwater defense technology is very important for a country in keeping and maintaining its marine wealth. This underwater robot is usually called the Remotely Operated Underwater Vehicle (ROV). The ROV is commonly used for marine security systems, assisting evaluation on at-sea accidents, and underwater exploration [1]. The ROV has two kinds of motions, namely, the translational and rotation motions on the x-, y-, and z-axes. Two parts of the ROV functioning to control the ROV motion are the propulsion system and the fin system. The propulsion system is used to regulate the angular velocity of the ROV, and the fin system is used to adjust the angle of the fin and the rudder position. The development of the ROV was initiated in the 1970s together with the initial investigation of the usefulness of the ROV system, and in 1970-1980, the ROV technology development and experiments were carried out. In 1980-1990, the experiments using prototypes were done, then in 1990-2000, the ICT-based ROV was developed.

This encouraged researches to improve the technology for innovations, in particular on the controller design of unmanned vehicles. The development of the controllers aimed to organize the actuator such that the unmanned vehicle can be stable in its motion as expected. Several studies related to the AUV control system began in the 2000s when Chiu et al. [2] used a fuzzy control sliding mode with a 2-DOF model. In 2002, W. Naeem [3] used a predictive control model for a nonlinear 2-DOF (surge and yaw) model. Kim and Ura [4] used the R-One Robot AUV with a length of 8.3 meters, a diameter of 1.2 meters, and a mass of 4400 kg with PID. Repoulias and Papadopoulos [5] used partial state-feedback in nonlinear 3-DOF (surge, sway and yaw) models. Lapierre and Soesanto [6] used the Infante AUV with a length of 4,215 m and a mass of 23 Kg with path-following control. Akcaya et al. [7] used SMC in a 3-DOF linear model. Rezazadegan et al. [8] used an adaptive nonlinear controller in the 5-DOF model. Oktafianto et al. [9] used SMC in the linear model of AUV. Herlambang et al. [10] used the PID controller method to control the movement of the 6-DOF linear model applied to UNUSAITS AUV, Nurhadi et al. [11] used the SMC method to control the Surge, Heave and Pitch Motions in the 3-DOF nonlinear model, in 2020, Herlambang et al. [12] used SPID Control in the 6-DOF linear model of the AUV, and also used the Linear Quadratic Regulator (LQR) for the linear motion system of the AUV [14].

The focus of this paper was to compare two control methods: SMC and SPID for 6-DOF motion control, of which the SPID controller is a combination of the SMC and PID controllers. This study used the 6-DOF liner model, and the linear model was obtained by linearization of the nonlinear 6-DOF model. The result of this study was the comparison of the stability performance of SMC and SPID shown by numerical simulation on the response results of both methods. The stability obtained by both methods was quite significant with an error of 0.1%-4% with a settling time of 0.1-1 second.

In order to analyze an ROV, it is necessary to consider the axis system which comprises the Earth Fixed Frame (EFF) and Body Fixed Frame (BFF) that are displayed in Figure 1 [14]. The motion of the ROV has 6 degrees of freedom (6 DOF) comprising 3 degrees of freedom in the direction of translational motions on the x-, y-, and z-axes and 3 degrees of freedom in the rotational motions on the x-, y- and z-axes. The general description of an ROV with 6 DOF can be expressed in (1), where $\_$ represents the position and orientation vectors over the EFF and v represents the linear and angular

velocities over the BFF. The details have been described in [15].

2 Remotely Operated Underwater Vehicle (ROV)

In order to analyze an ROV, it is necessary to consider the axis system which comprises the Earth Fixed Frame (EFF) and Body Fixed Frame (BFF) that are displayed in Figure 1 [14]. The motion of the ROV has 6 degrees of freedom (6 DOF) comprising 3 degrees of freedom in the direction of translational motions on the x-, y-, and z-axes and 3 degrees of freedom in the rotational motions on the x-, y- and z-axes. The general description of an ROV with 6 DOF can be given as (1) [15]

$$\begin{aligned} \eta &= [\eta_1^T, \eta_2^T]^T, \quad \eta_1 = [x, y, z]^T, \quad \eta_2 = [\emptyset, \theta, \Psi]^T, \\ v &= [v_1^T, v_2^T]^T, \quad v_1 = [u, v, w]^T, \quad v_2 = [p, q, r]^T, \\ \tau &= [\tau_1^T, \tau_2^T]^T, \quad \tau_1 = [X, Y, Z]^T, \quad \tau_2 = [K, M, N]^T. \end{aligned} \tag{1}$$

This study uses the prototype of the Evacuation ROV, and the specifications of the Evacuation ROV are: the weight is 16 kg, the length is 2 meter and the diameter is 300 mm [15]. The properties of the Evacuation ROV are displayed in Figure 2 and Table 1.

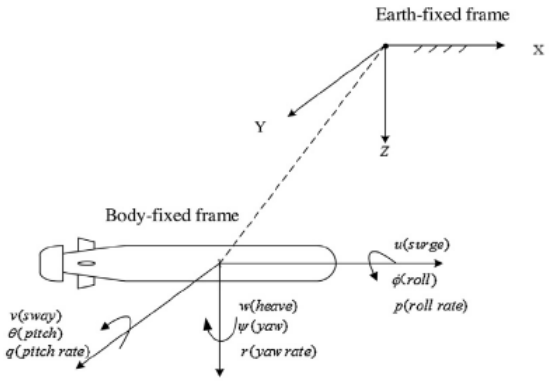

Figure 1: ROV Motion with Six Degrees of Freedom [20].

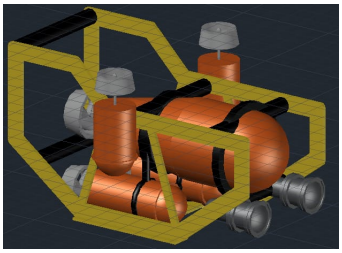

Figure 2: Profile of Evacuation ROV.

Table 1: Specification of the Evacuation ROV.

Weight	15 Kg
Overall Length	900 mm
Beam	300 mm
Controller	Wired Control ArduSUB with Joystick
Sensors	Depth Sensor, Sonar
Camera	TTL Camera
Lighting	1500 LM, 145° Beam Dimmable
Battery	11.8 V Li Po 5200 mAh
Material	Carbon Fiber
Main Propulsion	T200 Motor Thruster Include Propeller
Maneuver Propulsion	T200 Motor Thruster Include Propeller
Service Speed	1, 6 knots
Operation Depth	5 – 10 m

Variable η represents the vector position and orientation w.r.t. EFF, whereas τ represents the force vectors and moments that are working on the ROV w.r.t. BFF, namely surge (u), sway (v), heave (w), roll (p), pitch (q) and yaw (r). The total forces and moments which are working on the ROV can be gained by combining hydrostatic, hydrodynamic and thrust forces. In this case, we assumed that the diagonal inertia tensor (I_o) is zero, in order to obtain the total forces and moments of the whole model as follows.

Surge:

$$m[\dot{u} - vr + wq - x_G(q^2 + r^2) + y_G(pq - \dot{r}) + z_G(pr + \dot{q})] = X_{res} + X_{|u|u}u|u| + X_{\dot{u}}\dot{u} + X_{wq}wq + X_{qq}qq + X_{vr}vr + X_{rr}rr + X_{prop}, \quad (2)$$

Sway:

$$m[\dot{v} - wp + ur - y_G(r^2 + p^2) + z_G(qr - \dot{p}) + x_G(pq + \dot{r})] = Y_{res} + Y_{|v|v}v|v| + Y_{r|r|}r|r| + Y_{\dot{v}}\dot{v} + Y_{\dot{r}}\dot{r} + Y_{ur}ur + Y_{wp}wp + Y_{pq}pq + Y_{uv}uv + Y_{uu\delta_r}u^2\delta_r, \quad (3)$$

Heave:

$$m[\dot{w} - uq + vp - z_G(p^2 + q^2) + x_G(rp - \dot{q}) + y_G(rq + \dot{p})] = Z_{res} + Z_{|w|w}w|w| + Z_{q|q|}q|q| + Z_{\dot{w}}\dot{w} + Z_{\dot{q}}\dot{q} + Z_{uq}uq + Z_{vp}vp + Z_{rp}rp + Z_{uw}uw + Z_{uu\delta_s}u^2\delta_s, \quad (4)$$

Roll:

$$I_x\dot{p} + (I_z - I_y)qr + m[y_G(\dot{w} - uq + vp) - z_G(\dot{v} - wp + ur)]K_{res} + K_{p|p|}p|p| + K_{\dot{p}}\dot{p} + K_{prop}, \quad (5)$$

Pitch:

$$I_y\dot{q} + (I_x - I_z)rp + m[z_G(\dot{u} - vr + wq) - x_G(\dot{w} - uq + vp)] = M_{res} + M_{w|w|}w|w| + M_{q|q|}q|q| + M_{\dot{w}}\dot{w} + M_{\dot{q}}\dot{q} + M_{uq}uq + M_{vp}vp + M_{rp}rp + M_{uw}uw + M_{uu\delta_s}u^2\delta_s. \quad (6)$$

3 Linearization

In general, it is difficult to design a controller for nonlinear systems (2)-(6). Therefore, the non-linear ROV model is linearized by using the Jacobi matrix. The general equations of the non-linear ROV model can be written as

$$\begin{aligned} \dot{x}(t) &= f(x(t), u(t), t), \\ y(t) &= g(x(t), u(t), t), \end{aligned} \tag{7}$$

and the Jacobi matrix is defined as

$$\frac{\partial f(\bar{x}, \bar{u}, t)}{\partial x} = \begin{bmatrix} \frac{\partial f_1(\bar{x},\bar{u},t)}{\partial x_1} & \frac{\partial f_1(\bar{x},\bar{u},t)}{\partial x_2} & \cdots & \frac{\partial f_1(\bar{x},\bar{u},t)}{\partial x_n} \\ \frac{\partial f_2(\bar{x},\bar{u},t)}{\partial x_1} & \frac{\partial f_2(\bar{x},\bar{u},t)}{\partial x_2} & \cdots & \frac{\partial f_2(\bar{x},\bar{u},t)}{\partial x_n} \\ \vdots & \vdots & \ddots & \vdots \\ \frac{\partial f_n(\bar{x},\bar{u},t)}{\partial x_1} & \frac{\partial f_n(\bar{x},\bar{u},t)}{\partial x_2} & \cdots & \frac{\partial f_n(\bar{x},\bar{u},t)}{\partial x_n} \end{bmatrix}. \tag{8}$$

When the Jacobi matrix shown in (8) is used to linearize the ROV equation of motion for 6-DOF, then we obtain the following equation:

$$\frac{\partial f(\bar{x}, \bar{u}, t)}{\partial x} = \begin{bmatrix} \frac{\partial f_1(\bar{x},\bar{u},t)}{\partial u} & \frac{\partial f_1(\bar{x},\bar{u},t)}{\partial v} & \frac{\partial f_1(\bar{x},\bar{u},t)}{\partial w} & \frac{\partial f_1(\bar{x},\bar{u},t)}{\partial p} & \frac{\partial f_1(\bar{x},\bar{u},t)}{\partial q} & \frac{\partial f_1(\bar{x},\bar{u},t)}{\partial r} \\ \frac{\partial f_2(\bar{x},\bar{u},t)}{\partial u} & \frac{\partial f_2(\bar{x},\bar{u},t)}{\partial v} & \frac{\partial f_2(\bar{x},\bar{u},t)}{\partial w} & \frac{\partial f_2(\bar{x},\bar{u},t)}{\partial p} & \frac{\partial f_2(\bar{x},\bar{u},t)}{\partial q} & \frac{\partial f_2(\bar{x},\bar{u},t)}{\partial r} \\ \frac{\partial f_3(\bar{x},\bar{u},t)}{\partial u} & \frac{\partial f_3(\bar{x},\bar{u},t)}{\partial v} & \frac{\partial f_3(\bar{x},\bar{u},t)}{\partial w} & \frac{\partial f_3(\bar{x},\bar{u},t)}{\partial p} & \frac{\partial f_3(\bar{x},\bar{u},t)}{\partial q} & \frac{\partial f_3(\bar{x},\bar{u},t)}{\partial r} \\ \frac{\partial f_4(\bar{x},\bar{u},t)}{\partial u} & \frac{\partial f_4(\bar{x},\bar{u},t)}{\partial v} & \frac{\partial f_4(\bar{x},\bar{u},t)}{\partial w} & \frac{\partial f_4(\bar{x},\bar{u},t)}{\partial p} & \frac{\partial f_4(\bar{x},\bar{u},t)}{\partial q} & \frac{\partial f_4(\bar{x},\bar{u},t)}{\partial r} \\ \frac{\partial f_5(\bar{x},\bar{u},t)}{\partial u} & \frac{\partial f_5(\bar{x},\bar{u},t)}{\partial v} & \frac{\partial f_5(\bar{x},\bar{u},t)}{\partial w} & \frac{\partial f_5(\bar{x},\bar{u},t)}{\partial p} & \frac{\partial f_5(\bar{x},\bar{u},t)}{\partial q} & \frac{\partial f_5(\bar{x},\bar{u},t)}{\partial r} \\ \frac{\partial f_6(\bar{x},\bar{u},t)}{\partial u} & \frac{\partial f_6(\bar{x},\bar{u},t)}{\partial v} & \frac{\partial f_6(\bar{x},\bar{u},t)}{\partial w} & \frac{\partial f_6(\bar{x},\bar{u},t)}{\partial p} & \frac{\partial f_6(\bar{x},\bar{u},t)}{\partial q} & \frac{\partial f_6(\bar{x},\bar{u},t)}{\partial r} \end{bmatrix}, \tag{9}$$

where the functions f_1, f_2, f_3, f_4, f_5 and f_6 are

$$\begin{aligned} f_1 = \{&X_{res} + X_{|u|u}u|u| + X_{wq}wq + X_{qq}qq + X_{vr}vr + X_{rr}rr + X_{prop} - m[-vr + \\ &wq - x_G(q^2 + r^2) + pqy_G + prz_G]\}/\{m - X_{\dot{u}}\}, \end{aligned} \tag{10}$$

$$\begin{aligned} f_2 = \{&Y_{res} + Y_{|v|v}v|v| + Y_{r|r|}r|r| + Y_{\dot{r}}\dot{r} + Y_{ur}ur + Y_{wp}wp + Y_{pq}pq + Y_{uv}uv + \\ &Y_{uu\delta_r}u^2\delta_r - m[-wp + ur - y_G(r^2 + p^2) + qr\ z_G + pq\ x_G]\}/\{m - Y_{\dot{v}}\}, \end{aligned} \tag{11}$$

$$\begin{aligned} f_3 = \{&Z_{res} + Z_{|w|w}w|w| + Z_{q|q|}q|q| + Z_{\dot{q}}\dot{q} + Z_{uq}uq + Z_{vp}vp + Z_{rp}rp + Z_{uw}uw + \\ &Z_{uu\delta_s}u^2\delta_s - m[-uq + vp - z_G(p^2 + q^2) + rp\ x_G + rq\ y_G]\}/\{m - Z_{\dot{w}}\}, \end{aligned} \tag{12}$$

$$f_4 = \frac{K_{res} + K_{p|p|}p|p| + K_{prop} - ((I_z - I_y)qr + m[y_G(-uq + vp) - z_G(-wp + ur)])}{I_x - K_{\dot{p}}}, \tag{13}$$

$$\begin{aligned} f_5 = \{&M_{res} + M_{w|w|}w|w| + M_{q|q|}q|q| + M_{\dot{w}}\dot{w} + M_{uq}uq + M_{vp}vp + M_{rp}rp + M_{uw}uw + \\ &M_{uu\delta_s}u^2\delta_s - ((I_x - I_z)rp + m[z_G(-vr + wq) - x_G(-uq + vp)])\}/\{I_y - M_{\dot{q}}\}, \end{aligned} \tag{14}$$

$$\begin{aligned} f_6 = \{&N_{res} + N_{v|v|}v|v| + N_{r|r|}r|r| + N_{\dot{v}}\dot{v} + N_{ur}ur + N_{wp}wp + N_{pq}pq + N_{uv}uv + \\ &N_{uu\delta_r}u^2\delta_r - ((I_y - I_z)pq + m[x_G(-wp + ur) - y_G(-vr + wq)])\}/\{I_z - N_{\dot{r}}\}. \end{aligned} \tag{15}$$

The linear model obtained from the above process is as follows:

$$\begin{aligned} \dot{x}(t) &= Ax(t) + Bu(t), \\ y(t) &= Cx(t) + Du(t), \end{aligned} \tag{16}$$

where

$$A = J_x = \begin{bmatrix} 1 & 0 & 0 & 0 & \frac{mz_G}{m-X_{\dot{u}}} & \frac{-my_G}{m-X_{\dot{u}}} \\ 0 & 1 & 0 & -\frac{mz_G}{m-Y_{\dot{v}}} & 0 & \frac{(mx_G-Y_{\dot{r}})}{m-Y_{\dot{v}}} \\ 0 & 0 & 1 & \frac{my_G}{m-Z_{\dot{w}}} & -\frac{(mx_G+Z_{\dot{q}})}{m-Z_{\dot{w}}} & 0 \\ 0 & -\frac{m\ z_G}{I_x-K_{\dot{p}}} & \frac{m\ y_G}{I_x-K_{\dot{p}}} & 1 & 0 & 0 \\ \frac{m\ z_G}{I_y-M_{\dot{q}}} & 0 & -\frac{(m\ x_G+M_{\dot{w}})}{I_y-M_{\dot{q}}} & 0 & 1 & 0 \\ -\frac{my_G}{I_z-N_{\dot{r}}} & \frac{(mx_G-N_{\dot{v}})}{I_z-N_{\dot{r}}} & 0 & 0 & 0 & 1 \end{bmatrix}^{-1} \times \begin{bmatrix} a_1 & b_1 & c_1 & d_1 & e_1 & g_1 \\ a_2 & b_2 & c_2 & d_2 & e_2 & g_2 \\ a_3 & b_3 & c_3 & d_3 & e_3 & g_3 \\ a_4 & b_4 & c_4 & d_4 & e_4 & g_4 \\ a_5 & b_5 & c_5 & d_5 & e_5 & g_5 \\ a_6 & b_6 & c_6 & d_6 & e_6 & g_6 \end{bmatrix},$$

$$B = J_u = \begin{bmatrix} 1 & 0 & 0 & 0 & \frac{mz_G}{m-X_{\dot{u}}} & \frac{-my_G}{m-X_{\dot{u}}} \\ 0 & 1 & 0 & -\frac{mz_G}{m-Y_{\dot{v}}} & 0 & \frac{(mx_G-Y_{\dot{r}})}{m-Y_{\dot{v}}} \\ 0 & 0 & 1 & \frac{my_G}{m-Z_{\dot{w}}} & -\frac{(mx_G+Z_{\dot{q}})}{m-Z_{\dot{w}}} & 0 \\ 0 & -\frac{m\ z_G}{I_x-K_{\dot{p}}} & \frac{m\ y_G}{I_x-K_{\dot{p}}} & 1 & 0 & 0 \\ \frac{m\ z_G}{I_y-M_{\dot{q}}} & 0 & -\frac{(m\ x_G+M_{\dot{w}})}{I_y-M_{\dot{q}}} & 0 & 1 & 0 \\ -\frac{my_G}{I_z-N_{\dot{r}}} & \frac{(mx_G-N_{\dot{v}})}{I_z-N_{\dot{r}}} & 0 & 0 & 0 & 1 \end{bmatrix}^{-1} \times \begin{bmatrix} A_1 & B_1 & C_1 & D_1 & E_1 & G_1 \\ A_2 & B_2 & C_2 & D_2 & E_2 & G_2 \\ A_3 & B_3 & C_3 & D_3 & E_3 & G_3 \\ A_4 & B_4 & C_4 & D_4 & E_4 & G_4 \\ A_5 & B_5 & C_5 & D_5 & E_5 & G_5 \\ A_6 & B_6 & C_6 & D_6 & E_6 & G_6 \end{bmatrix},$$

$$C = \begin{bmatrix} 1 & 0 & 0 & 0 & 0 & 0 \\ 0 & 1 & 0 & 0 & 0 & 0 \\ 0 & 0 & 1 & 0 & 0 & 0 \\ 0 & 0 & 0 & 1 & 0 & 0 \\ 0 & 0 & 0 & 0 & 1 & 0 \\ 0 & 0 & 0 & 0 & 0 & 1 \end{bmatrix}, D = 0.$$

4 Sliding Mode Control

SMC is a controller that is robust w.r.t. internal and external disturbances. As such, SMC has been widely used in many applications. In order to apply SMC to a system, we need to proceed according to the algorithm presented in Figure 3.

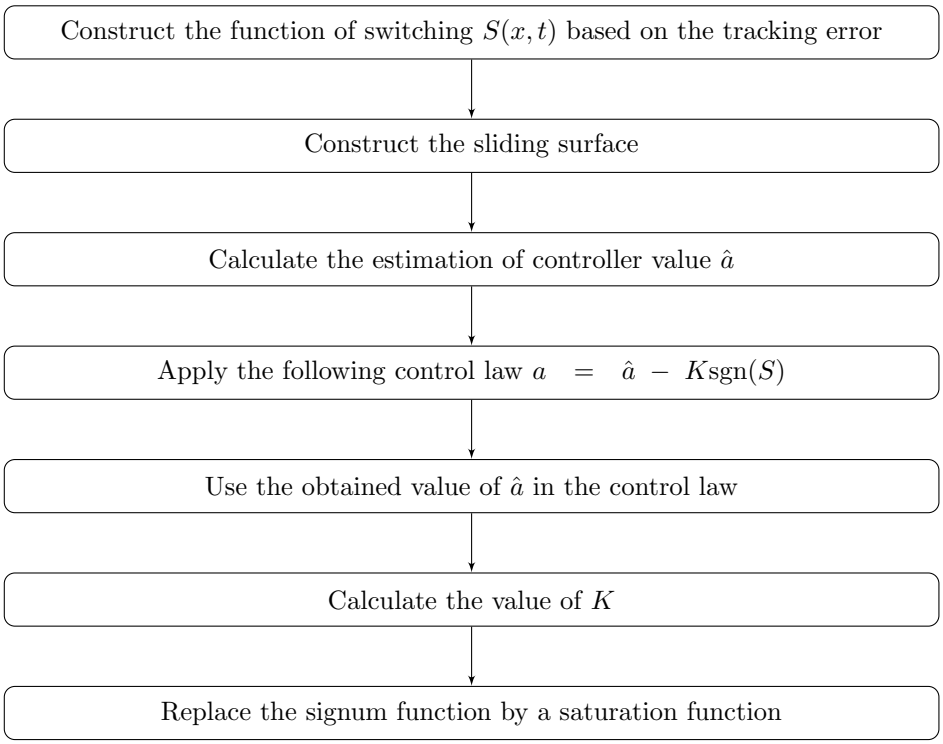

Figure 3: Algorithm of Sliding Mode Control.

5 Sliding PID

The design of the Sliding-PID control system is a combination of SMC and PID. In this study, the system first passes through SMC, then the result is optimized by the PID controller. The process works as follows. The notation e represents the error signal, i.e., the difference between the output and the reference. The error signal is substituted into the sliding surface equation $S = \dot{e} + \lambda e$ for some $\lambda \in \mathbb{R}$. Then the value of S is used by the PID to determine the input signal u. This scheme is shown in the block diagram in Figure 4.

6 Control System Design

Designing the SMC control system for the 6-DOF linear model involves creating control equations for surge, sway, heave, roll, pitch and yaw, obtained by the SMC Algorithm

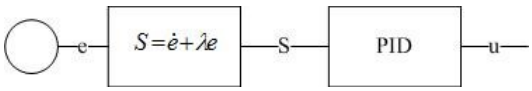

Figure 4: Block Diagram of SPID.

described in the previous section. From (16), the status of surge can be written as follows:

$$\dot{u} = aa_1u + bb_1v + cc_1w + dd_1p + ee_1q + gg_1r + AA_1X_{prop} + BB_1\delta_{r_1} + CC_1\delta_{s_1} + DD_1K_{prop} + EE_1\delta_{s_2} + GG_1\delta_{r_2}. \quad (17)$$

To find the control of the surge, the tracking error of surge is determined as follows:

$$\tilde{u} = u - u_d,$$

where u_d is a constant function. Since the system has order 1, the switching function is formed as follows:

$$S(u,t) = \left(\frac{d}{dt}\right)^{n-1} \tilde{u}, \quad \text{with } n = 1,$$
$$S(u,t) = \left(\frac{d}{dt}\right)^{1-1} \tilde{u},$$
$$S(u,t) = \tilde{u} = u - u_d.$$

The derivative of S is

$$\dot{S}(u,t) = \dot{u} - \dot{u}_d. \quad (18)$$

Since u_d is a constant function, one has $\dot{u}_d = 0$. By subtituting the equation (17) into (18), we get

$$\dot{S}(u,t) = aa_1u + bb_1v + cc_1w + dd_1p + ee_1q + gg_1r + AA_1X_{prop} + BB_1\delta_{r_1} + CC_1\delta_{s_1} + DD_1K_{prop} + EE_1\delta_{s_2} + GG_1\delta_{r_2}. \quad (19)$$

Next, the value of $\hat{X}_{prop}$ is determined from the equation (19), when the value of $\dot{S} = 0$, as follows:

$$aa_1u + bb_1v + cc_1w + dd_1p + ee_1q + gg_1r + AA_1X_{prop} + BB_1\delta_{r_1} + CC_1\delta_{s_1} + DD_1K_{prop} + EE_1\delta_{s_2} + GG_1\delta_{r_2} = 0. \quad (20)$$

Then the obtained $\hat{X}_{prop}$ is

$$\hat{X}_{prop} = -\left(\frac{aa_1u + bb_1v + cc_1w + dd_1p + ee_1q + gg_1r}{AA_1}\right) - \left(\frac{BB_1\delta_{r_1} + CC_1\delta_{s_1} + DD_1K_{prop} + EE_1\delta_{s_2} + GG_1\delta_{r_2}}{AA_1}\right). \quad (21)$$

Since we require that the control law has to satisfy the condition of sliding, we have

$$X_{prop} = \hat{X}_{prop} - K_1\text{sgn}(S), \quad (22)$$

then from the equation (21) and (22), it is obtained that

$$X_{prop} = -\left(\frac{aa_1u + bb_1v + cc_1w + dd_1p + ee_1q + gg_1r}{AA_1}\right) - \left(\frac{BB_1\delta_{r_1} + CC_1\delta_{s_1} + DD_1K_{prop} + EE_1\delta_{s_2} + GG_1\delta_{r_2}}{AA_1}\right) - K_1\text{sgn}(S). \quad (23)$$

By substituting the equation (23) into (19), it is obtained that

$$\dot{S}(u,t) = -AA_1K_1\text{sgn}(S). \quad (24)$$

Next, the value of K_1 is set up by substituting the equation (24) into the following equation to meet the sliding condition, that is,

$$S\dot{S} \leq -\eta|S|, \quad (25)$$

$$-SAA_1K_1\text{sgn}(S) \leq -\eta|S|,$$

$$-AA_1K_1\text{sgn}(S) \leq -\frac{\eta|S|}{S,}$$

$$K_1 \geq \frac{\eta}{AA_1\text{sgn}(S)}. \quad (26)$$

From the equation (26), the value of K_1 is obtained as follows:

$$K_1 = \left|\max\frac{\eta}{AA_1}\right|. \quad (27)$$

Next, in order to minimize chattering, a boundary layer is used by replacing the function of signum (sgn) into the function of saturation (sat) as follows:

$$X_{prop} = \hat{X}_{prop} - K_1\text{sat}\left(\frac{S}{\phi}\right). \quad (28)$$

Thus, the design of the SMC control of surge, obtained by substituting the equations (21) and (27) into the equation (28), is as follows:

$$X_{prop} = -\left(\frac{aa_1u + bb_1v + cc_1w + dd_1p + ee_1q + gg_1r + BB_1\delta_{r_1} + CC_1\delta_{s_1} + DD_1K_{prop} + EE_1\delta_{s_2}}{AA_1}\right) - \frac{GG_1\delta_{r_2}}{AA_1} - \left|\max\frac{\eta}{AA_1}\right| \text{ sat}\left(\frac{S}{\phi}\right). \quad (29)$$

Furthermore, the state equations for sway, heave, roll, pitch and yaw are as follows:

$$\dot{v} = aa_2u + bb_2v + cc_2w + dd_2p + ee_2q + gg_2r + AA_2X_{prop} + BB_2\delta_{r_1} + CC_2\delta_{s_1} + DD_2K_{prop} + EE_2\delta_{s_2} + GG_2\delta_{r_2} \quad (30)$$

$$\dot{w} = aa_3u + bb_3v + cc_3w + dd_3p + ee_3q + gg_3r + AA_3X_{prop} + BB_3\delta_{r_1} + CC_3\delta_{s_1} + DD_3K_{prop} + EE_3\delta_{s_2} + GG_3\delta_{r_2} \quad (31)$$

$$\dot{p} = aa_4u + bb_4v + cc_4w + dd_4p + ee_4q + gg_4r + AA_4X_{prop} + BB_4\delta_{r_1} + CC_4\delta_{s_1} + DD_4K_{prop} + EE_4\delta_{s_2} + GG_4\delta_{r_2} \quad (32)$$

$$\dot{q} = aa_5u + bb_5v + cc_5w + dd_5p + ee_5q + gg_5r + AA_3X_{prop} + BB_5\delta_{r_1} + CC_5\delta_{s_1} + DD_5K_{prop} + EE_5\delta_{s_2} + GG_5\delta_{r_2} \quad (33)$$

$$\dot{r} = aa_6u + bb_6v + cc_6w + dd_6p + ee_6q + gg_6r + AA_6X_{prop} + BB_6\delta_{r_1} + CC_6\delta_{s_1} + DD_6K_{prop} + EE_6\delta_{s_2} + GG_6\delta_{r_2}. \quad (34)$$

In the same way as obtaining the surge input control with the switching function, control law, sliding conditions and applying the boundary layer, the input controls for sway, heave, roll, pitch and yaw are as follows:

$$\delta_{r_1} = -\left(\frac{aa_2u + bb_2v + cc_2w + dd_2p + ee_2q + gg_2r}{BB_2}\right) - \left(\frac{AA_2X_{prop} + CC_2\delta_{s_1} + DD_2K_{prop} + EE_2\delta_{s_2} + GG_2\delta_{r_2}}{BB_2}\right) - \left|\max\frac{\eta}{BB_2}\right| \text{sat}\left(\frac{S}{\phi}\right), \tag{35}$$

$$\delta_{s_1} = -\left(\frac{aa_3u + bb_3v + cc_3w + dd_3p + ee_3q + gg_3r}{CC_3}\right) - \left(\frac{AA_3X_{prop} + BB_3\delta_{r_1} + DD_3K_{prop} + EE_3\delta_{s_2} + GG_3\delta_{r_2}}{CC_3}\right) - \left|\max\frac{\eta}{CC_3}\right| \text{sat}\left(\frac{S}{\phi}\right), \tag{36}$$

$$K_{prop} = -\left(\frac{aa_4u + bb_4v + cc_4w + dd_4p + ee_4q + gg_4r}{DD_4}\right) - \left(\frac{AA_4X_{prop} + BB_4\delta_{r_1} + CC_4\delta_{s_1} + EE_4\delta_{s_2} + GG_4\delta_{r_2}}{DD_4}\right) - \left|\max\frac{\eta}{AA_1}\right| \text{sat}\left(\frac{S}{\phi}\right), \tag{37}$$

$$\delta_{s_2} = -\left(\frac{aa_5u + bb_5v + cc_5w + dd_5p + ee_5q + gg_5r}{EE_5}\right) - \left(\frac{AA_3X_{prop} + BB_5\delta_{r_1} + CC_5\delta_{s_1} + DD_5K_{prop} + GG_5\delta_{r_2}}{EE_5}\right) - \left|\max\frac{\eta}{CC_3}\right| \text{sat}\left(\frac{S}{\phi}\right), \tag{38}$$

$$\delta_{r_2} = -\left(\frac{aa_6u + bb_6v + cc_6w + dd_6p + ee_6q + gg_6r}{GG_6}\right) - \left(\frac{AA_6X_{prop} + BB_6\delta_{r_1} + CC_6\delta_{s_1} + DD_6K_{prop} + EE_6\delta_{s_2}}{GG_6}\right) - \left|\max\frac{\eta}{BB_2}\right| \text{sat}\left(\frac{S}{\phi}\right). \tag{39}$$

The design of the SPID control system for the 6-DOF linear model first passes the SMC control system equation, then the result is optimized by the PID controller whose proportional, integral and derivative values are shown in Table 2. Once the control system equations are obtained, they are connected to the 6-DOF linear model on the block diagram shown in Figure 5 (right).

Table 2: Proportional, Integral and Derivative Values of SPID.

	K_p	K_i	K_d
Surge	2.1	0	0
Sway	2.01	0	0
Heave	2.01	0	0
Roll	2.01	0	0
Pitch	2.1	0	0
Yaw	2.1	0	0

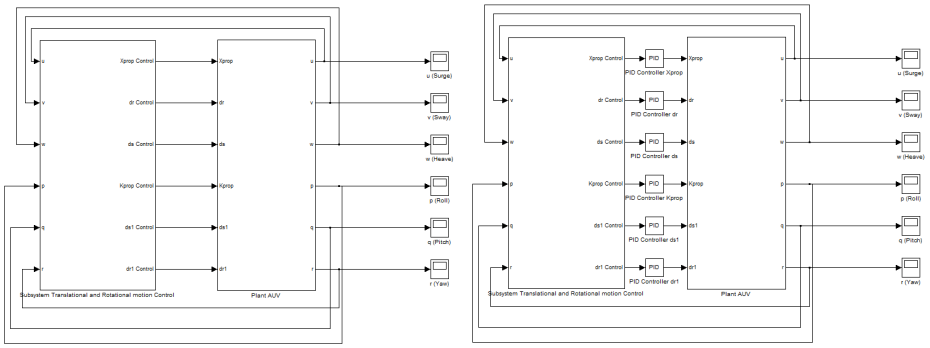

Figure 5: The Left Panel Displays the ROV Block Diagram Using the SMC Control System. The Right Panel Displays the ROV Block Diagram Using the SPID Control System.

7 Computational Results

In the simulation, the response ratio of SMC and SPID control systems for surge, sway, heave, roll, pitch and yaw motion was obtained. The setpoint of surge is 1 m/s, those of sway and heave are 1 m/s, while the setpoint for roll rotation motion is 1 rad/s, and those of pitch and yaw are -1 rad/s. From the simulation results, the comparison of time delay, rise time, peak time and settling time was obtained. The simulation results by SMC and SPID control systems are shown in Figure 6.

The comparison of the surge responses in Figure 6 (top left) is the result of AUV simulation by SMC and SPID control systems. The results of both methods show similarity of the delay time of 0.03 s, the rise time of 0.05 s, the peak time of 0.08 s, and the settling time of 1 s. SMC and SPID are stable at the setpoint of 1 m/s at time of 1 s. When viewed from the resulted error, SPID is 3.4%, while SMC is 4.15%. Figure 6 (top right) shows the similarities for the delay time, rise time, peak time and settling time. That is, the delay time is 0.037 s, the rise time is 0.065 s, the peak time is 0.07 s, and the settling time is 0.1 s. SMC and SPID are stable at the setpoint -1 m/s at 0.1 s. In terms of the resulted error, that of SPID is 0.09% and that of SMC is 0.11%. In Figure 6 (middle left), it is shown that the results of both methods have similarity for a delay time, that is, a delay time of 0.037 s. SMC has a rise time of 0.15 s and a settling time of 0.2 s, while SPID has a rise time of 0.25 s and a settling time of 0.25 s. SMC and SPID are stable at the setpoint 1 m/s at 0.2 s. SMC and SPID on the heave response do not have a peak time and maximum overshoot. As regards the error generated, that of SMC is 0.19% and that of SPID is 0.8%.

The comparison of the roll response in Figure 6 (middle right) is the result of the simulation of the AUV with SMC and SPID control systems. The results of both methods show similarity of a delay time of 0.04 s, rise time of 0.12 s, and settling time of 0.12 s. The response generated by the SMC and SPID methods is stable at the setpoint 1 rad/s at 0.12 s. SMC and SPID on the roll response do not have a peak time and maximum overshoot. In terms of the error generated, that of SMC is 0.42%, while that of SPID is 0.6%, so SMC is better than SPID for the roll response. Figure 6 (bottom left) shows that the response results by SMC and SPID methods are stable at the setpoint -1 rad/s, the SMC settling time at 1.5 s, while that of SPID at 1.25 s. As regards the error generated, that of SPID is 4.3% while that of SMC is 4.58%, so SPID is better than SMC but it

has a higher overshoot. Figure 6 (bottom right) shows that the results of both methods show similarity in a delay time of 0.002 s, rise time of 0.082 s, peak time of 0.07 s, and settling time of 0.2 s. The results of SMC and SPID methods are stable at the setpoint -1 rad/s at 0.2 s. As regards the error generated, that of SMC is 3.66%, while that of SPID is 4.77%, so the the SMC method is better than the SPID one. And, the SMC method has a lower overshoot than the SPID one.

The comparison of delay time, rise time, peak time, maximum overshoot, settling time, and error in responses, respectively, by the default PID control system, identical PID, SMC and SPID is shown in Table 3 for surge, sway, heave response. Meanwhile, the comparison for responses in roll, pitch, and yaw is shown in Table 4. From this comparison of responses, it can be concluded that the best control system for the AUV is seen from the error and the settling time. The SPID method is more stable for the surge, sway and pitch motion, while the SMC method is more stable for the heave, roll and yaw motion. Next, it can be checked by making stability analysis using the Lyapunov method.

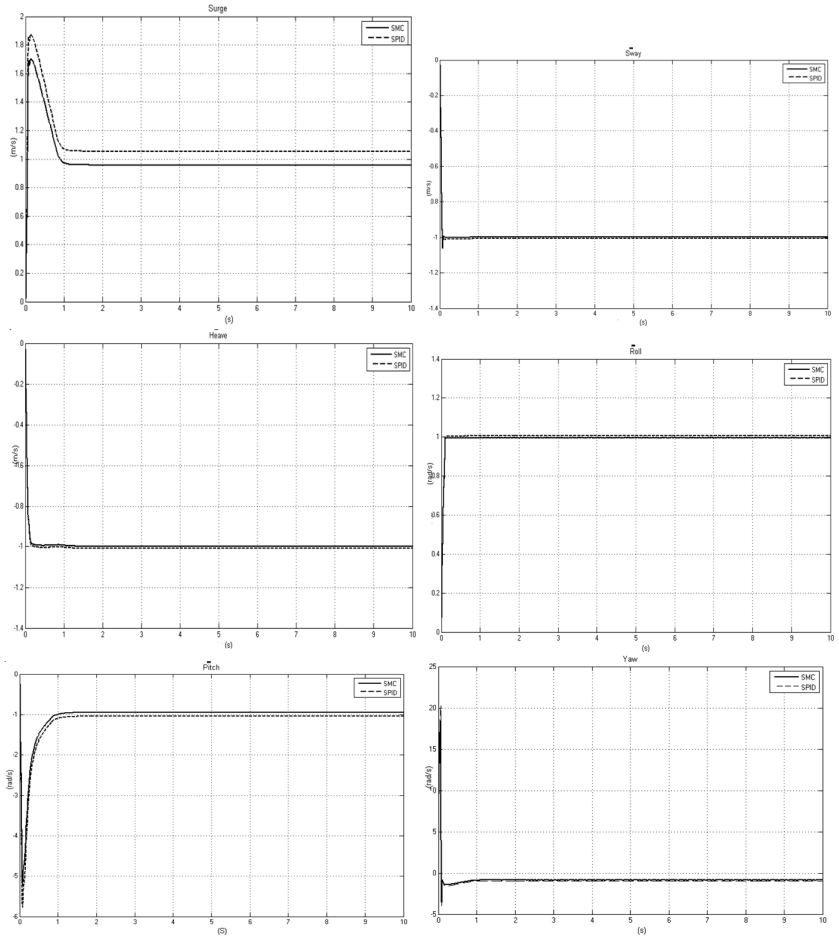

Figure 6: Response of the Surge, Sway, Heave, Roll, Pitch and Yaw Motions by Using SMC and SPID Control Systems.

Table 3: Specifications of the Transient Responses in the Surge, Sway, and Heave Motions.

	Surge		Sway		Heave	
	SMC	SPID	SMC	SPID	SMC	SPID
Delay Time	0.03 s	0.029 s	0.037 s	0.037 s	0.045 s	0.045 s
Rise Time	0.05 s	0.046 s	0.065 s	0.065 s	0.15 s	0.25 s
Peak Time	0.08 s	0.08 s	0.07 s	0.07 s	0 s	0 s
Maximum Peak	1.7 m/s	1.85 m/s	-1.1 m/s	-1.2 m/s	0 m/s	0 m/s
Settling Time	1 s	1 s	0.1 s	0.1 s	0.2 s	0.25 s
Error	4.15%	3.4%	0.11%	0.9%	0.19%	0.8%

Table 4: Specification of the Transient Responses in the Roll, Pitch, and Yaw Motions.

	Roll		Pitch		Yaw	
	SMC	SPID	SMC	SPID	SMC	SPID
Delay Time	0.04 s	0.04 s	0.01 s	0.01 s	0.002 s	0.002 s
Rise Time	0.12 s	0.12 s	0.2 s	0.2 s	0.082 s	0.082 s
Peak Time	0 s	0 s	0.075 s	0.074 s	0.07 s	0.07 s
Maximum Peak	0 m/s	0 m/s	-5.2 m/s	-5.8 m/s	18 m/s	21 m/s
Settling Time	0.12 s	0.12 s	1.5 s	1.25 s	0.2 s	0.2 s
Error	0.42%	0.6%	4.58%	4.3%	3.66%	4.77%

8 Stability Analysis

A candidate of the Lyapunov function for the ROV linear system with 6-DOF is

$$V(u,v,w,p,q,r) = \frac{1}{2}u^2 + \frac{1}{2}v^2 + \frac{1}{2}w^2 + \frac{1}{2}p^2 + \frac{1}{2}q^2 + \frac{1}{2}r^2. \tag{40}$$

We will show that $V(u,v,w,p,q,r)$ is a Lyapunov function that satisfies the stability criteria.

For the Lyapunov candidate function in equation (40), it will be proven that the candidate function with the SMC and SPID control system in the linear model is the Lyapunov function and the equilibrium point is asymptotically stable.

1. For $(u,v,w,p,q,r) = (0,0,0,0,0,0)$, we obtain $V(u,v,w,p,q,r) = 0$, whereas for $(u,v,w,p,q,r) \neq (0,0,0,0,0,0)$, we obtain $V(u,v,w,p,q,r) > 0$. Then $V(u,v,w,p,q,r)$ has been proven to be positive definite for SMC and SPID.

2. The function V is continuous and it has a continuous first partial derivative at S. The function V in (40) is a quadratic function, then it is easy to see that the quadratic function is continuous. As a consequence, the partial derivative is also continuous.

3. The third requirement of the SMC method is as follows:

$$\begin{aligned}\dot{V}(u,v,w,p,q,r) &= \frac{\partial V}{\partial u}\dot{u} + \frac{\partial V}{\partial v}\dot{v} + \frac{\partial V}{\partial w}\dot{w} + \frac{\partial V}{\partial p}\dot{p} + \frac{\partial V}{\partial q}\dot{q} + \frac{\partial V}{\partial r}\dot{r} \\ &= u\dot{u} + v\dot{v} + w\dot{w} + p\dot{p} + q\dot{q} + r\dot{r} \\ &= u(aa_1u + bb_1v + cc_1w + dd_1p + ee_1q + gg_1r + AA_1X_{prop} + BB_1\delta_{r_1} + \\ &\quad CC_1\delta_{s_1} + DD_1K_{prop} + EE_1\delta_{s_2} + GG_1\delta_{r_2}) + v(aa_2u + bb_2v + cc_2w + \\ &\quad dd_2p + ee_2q + gg_2r + AA_2X_{prop} + BB_2\delta_{r_1} + CC_2\delta_{s_1} + DD_2K_{prop} + \\ &\quad EE_2\delta_{s_2} + GG_2\delta_{r_2}) + w(aa_3u + bb_3v + cc_3w + dd_3p + ee_3q + gg_3r + \\ &\quad AA_3X_{prop} + BB_3\delta_{r_1} + CC_3\delta_{s_1} + DD_3K_{prop} + EE_3\delta_{s_2} + GG_3\delta_{r_2}) + \\ &\quad p(aa_4u + bb_4v + cc_4w + dd_4p + ee_4q + gg_4r + AA_4X_{prop} + BB_4\delta_{r_1} + \\ &\quad CC_4\delta_{s_1} + DD_4K_{prop} + EE_4\delta_{s_2} + GG_4\delta_{r_2}) + q(aa_5u + bb_5v + cc_5w + \\ &\quad dd_5p + ee_5q + gg_5r + AA_3X_{prop} + BB_5\delta_{r_1} + CC_5\delta_{s_1} + DD_5K_{prop} + \\ &\quad EE_5\delta_{s_2} + GG_5\delta_{r_2}) + r(aa_6u + bb_6v + cc_6w + dd_6p + ee_6q + gg_6r + \\ &\quad AA_6X_{prop} + BB_6\delta_{r_1} + CC_6\delta_{s_1} + DD_6K_{prop} + EE_6\delta_{s_2} + GG_6\delta_{r_2}).\end{aligned} \tag{41}$$

We take

$$\begin{aligned}X_{prop} = &-\left(\frac{aa_1u + bb_1v + cc_1w + dd_1p + ee_1q + gg_1r}{AA_1}\right) - \\ &\left(\frac{BB_1\delta_{r_1} + CC_1\delta_{s_1} + DD_1K_{prop} + EE_1\delta_{s_2} + GG_1\delta_{r_2}}{AA_1}\right) - K_1\text{sgn}(S),\end{aligned} \tag{42}$$

$$\begin{aligned}\delta_{r_1} = &-\left(\frac{aa_2u + bb_2v + cc_2w + dd_2p + ee_2q + gg_2r}{BB_2}\right) - \\ &\left(\frac{AA_2X_{prop} + CC_2\delta_{s_1} + DD_2K_{prop} + EE_2\delta_{s_2} + GG_2\delta_{r_2}}{BB_2}\right) - K_2\text{sgn}(S),\end{aligned} \tag{43}$$

$$\begin{aligned}\delta_{s_1} = &-\left(\frac{aa_3u + bb_3v + cc_3w + dd_3p + ee_3q + gg_3r}{CC_3}\right) - \\ &\left(\frac{AA_3X_{prop} + BB_3\delta_{r_1} + DD_3K_{prop} + EE_3\delta_{s_2} + GG_3\delta_{r_2}}{CC_3}\right) - K_3\text{sgn}(S),\end{aligned} \tag{44}$$

$$\begin{aligned}K_{prop} = &-\left(\frac{aa_4u + bb_4v + cc_4w + dd_4p + ee_4q + gg_4r}{DD_4}\right) - \\ &\left(\frac{AA_4X_{prop} + BB_4\delta_{r_1} + CC_4\delta_{s_1} + EE_4\delta_{s_2} + GG_4\delta_{r_2}}{DD_4}\right) - K_4\text{sgn}(S),\end{aligned} \tag{45}$$

$$\delta_{s_2} = -\left(\frac{aa_5u + bb_5v + cc_5w + dd_5p + ee_5q + gg_5r}{EE_5}\right) - \left(\frac{AA_3X_{prop} + BB_5\delta_{r_1} + CC_5\delta_{s_1} + DD_5K_{prop} + GG_5\delta_{r_2}}{EE_5}\right) - K_5\text{sgn}(S), \tag{46}$$

$$\delta_{r_2} = -\left(\frac{aa_6u + bb_6v + cc_6w + dd_6p + ee_6q + gg_6r}{GG_6}\right) - \left(\frac{AA_6X_{prop} + BB_6\delta_{r_1} + CC_6\delta_{s_1} + DD_6K_{prop} + EE_6\delta_{s_2}}{GG_6}\right) - K_6\text{sgn}(S). \tag{47}$$

Substitute equations (42)-(47) into equation (41), then we obtain

$$\begin{aligned}\dot{V}(u,v,w,p,q,r) = {} & u(-AA_1K_1\text{sgn}(S)) + v(-BB_2K_2\text{sgn}(S)) + w(-CC_3K_3\text{sgn}(S)) + \\ & p(-DD_4K_4\text{sgn}(S)) + q(-EE_5K_5\text{sgn}(S)) + r(-GG_6K_6\text{sgn}(S)) \leq \\ & (-AA_1K_1)u + (-BB_2K_2)v + (-CC_3K_3)w + (-DD_4K_4)p + \\ & (-EE_5K_5)q + (-GG_6K_6)r.\end{aligned}$$

We take $K_1 = \left|\frac{1}{AA_1}\right|\eta$, $K_2 = \left|\frac{1}{BB_2}\right|\eta$, $K_3 = \left|\frac{1}{CC_3}\right|\eta$, $K_4 = \left|\frac{1}{DD_4}\right|\eta$, $K_5 = \left|\frac{1}{EE_5}\right|\eta$, $K_6 = \left|\frac{1}{GG_6}\right|\eta$. Then we obtain

$$\begin{aligned}\dot{V}(u,v,w,p,q,r) &\leq (-\eta)|u| + (-\eta)|v| + (-\eta)|w| + (-\eta)|p| + (-\eta)|q| + (-\eta)|r| \\ &\leq -\eta(|u| + |v| + |w| + |p| + |q| + |r|).\end{aligned}$$

From the above requirements, the function V is the function of Lyapunov and the system is asymptotically stable.

The third characteristics of the SPID method is as follows:

$$X_{prop} = -\left(\frac{aa_1u + bb_1v + cc_1w + dd_1p + ee_1q + gg_1r}{AA_1}\right) - \left(\frac{BB_1\delta_{r_1} + CC_1\delta_{s_1} + DD_1K_{prop} + EE_1\delta_{s_2} + GG_1\delta_{r_2}}{AA_1}\right) + \left(K_{p1}u + K_{i1}\frac{1}{2}u^2 + K_{d1}\dot{u}\right), \tag{48}$$

$$\delta_{r_1} = -\left(\frac{aa_2u + bb_2v + cc_2w + dd_2p + ee_2q + gg_2r}{BB_2}\right) - \left(\frac{AA_2X_{prop} + CC_2\delta_{s_1} + DD_2K_{prop} + EE_2\delta_{s_2} + GG_2\delta_{r_2}}{BB_2}\right) +$$

$$\left(K_{p2}v + K_{i2}\frac{1}{2}v^2 + K_{d2}\dot{v}\right), \tag{49}$$

$$\delta_{s_1} = -\left(\frac{aa_3u + bb_3v + cc_3w + dd_3p + ee_3q + gg_3r}{CC_3}\right) - \left(\frac{AA_3X_{prop} + BB_3\delta_{r_1} + DD_3K_{prop} + EE_3\delta_{s_2} + GG_3\delta_{r_2}}{CC_3}\right) + \left(K_{p3}w + K_{i3}\frac{1}{2}w^2 + K_{d3}\dot{w}\right), \tag{50}$$

$$K_{prop} = -\left(\frac{aa_4u + bb_4v + cc_4w + dd_4p + ee_4q + gg_4r}{DD_4}\right) - \left(\frac{AA_4X_{prop} + BB_4\delta_{r_1} + CC_4\delta_{s_1} + EE_4\delta_{s_2} + GG_4\delta_{r_2}}{DD_4}\right) + \left(K_{p4}p + K_{i4}\frac{1}{2}p^2 + K_{d4}\dot{p}\right), \tag{51}$$

$$\delta_{s_2} = -\left(\frac{aa_5u + bb_5v + cc_5w + dd_5p + ee_5q + gg_5r}{EE_5}\right) - \left(\frac{AA_3X_{prop}BB_5\delta_{r_1} + CC_5\delta_{s_1} + DD_5K_{prop} + GG_5\delta_{r_2}}{EE_5}\right) + \left(K_{p5}q + K_{i5}\frac{1}{2}q^2 + K_{d5}\dot{q}\right), \tag{52}$$

$$\delta_{r_2} = -\left(\frac{aa_6u + bb_6v + cc_6w + dd_6p + ee_6q + gg_6r}{GG_6}\right) - \left(\frac{AA_6X_{prop} + BB_6\delta_{r_1} + CC_6\delta_{s_1} + DD_6K_{prop} + EE_6\delta_{s_2}}{GG_6}\right) + \left(K_{p6}r + K_{i6}\frac{1}{2}r^2 + K_{d6}\dot{r}\right). \tag{53}$$

Then equations (48)-(53) will be substituted to X_{prop}, δ_{r_1}, δ_{s_1}, K_{prop}, δ_{s_2} and δ_{r_2} in equation (41). The following equation is obtained:

$$\begin{aligned}\dot{V}(u,v,w,p,q,r) = u&\left(\frac{aa_1u + bb_1v + cc_1w + dd_1p + ee_1q + gg_1r + AA_1(K_{p1}u + K_{i1}\frac{1}{2}u^2)}{1 - AA_1K_{d1}} + \right.\\ &\left.\frac{BB_1\delta_{r_1} + CC_1\delta_{s_1} + DD_1K_{prop} + EE_1\delta_{s_2} + GG_1\delta_{r_2}}{1 - AA_1K_{d1}}\right) +\\ v&\left(\frac{aa_2u + bb_2v + cc_2w + dd_2p + ee_2q + gg_2r + AA_2X_{prop}}{1 - BB_2K_{d2}} + \right.\\ &\left.\frac{BB_2(K_{p2}v + K_{i2}\frac{1}{2}v^2) + CC_2\delta_{s_1} + DD_2K_{prop} + EE_2\delta_{s_2} + GG_2\delta_{r_2}}{1 - BB_2K_{d2}}\right) +\\ w&\left(\frac{aa_3u + bb_3v + cc_3w + dd_3p + ee_3q + gg_3r + AA_3X_{prop}}{1 - CC_3K_{d3}} + \right.\\ &\left.\frac{BB_3\delta_{r_1} + CC_3(K_{p3}w + K_{i3}\frac{1}{2}w^2) + DD_3K_{prop} + EE_3\delta_{s_2} + GG_3\delta_{r_2}}{1 - CC_3K_{d3}}\right) +\end{aligned}$$

$$p\left(\frac{aa_4u+bb_4v+cc_4w+dd_4p+ee_4q+gg_4r+AA_4X_{prop}}{1-DD_4K_{d4}}\right.$$
$$\left.+\frac{BB_4\delta_{r_1}+CC_4\delta_{s_1}+DD_4(K_{p4}p+K_{i4}\frac{1}{2}p^2)+EE_4\delta_{s_2}+GG_4\delta_{r_2}}{1-DD_4K_{d4}}\right)+$$
$$q\left(\frac{aa_5u+bb_5v+cc_5w+dd_5p+ee_5q+gg_5r+AA_3X_{prop}}{1-EE_5K_{d5}}+\right.$$
$$\left.\frac{BB_5\delta_{r_1}+CC_5\delta_{s_1}+DD_5K_{prop}+EE_5(K_{p5}q+K_{i5}\frac{1}{2}q^2)+GG_5\delta_{r_2}}{1-EE_5K_{d5}}\right)+$$
$$r\left(\frac{aa_6u+bb_6v+cc_6w+dd_6p+ee_6q+gg_6r+AA_6X_{prop}+BB_6\delta_{r_1}}{1-GG_6K_{d6}}+\right.$$
$$\left.\frac{CC_6\delta_{s_1}+DD_6K_{prop}+EE_6\delta_{s_2}+GG_6(K_{p6}r+K_{i6}\frac{1}{2}r^2)}{1-GG_6K_{d6}}\right) \tag{54}$$

Next, we take

$$K_7=\left|aa_1u+bb_1v+cc_1w+dd_1p+ee_1q+gg_1r+AA_1\left(K_{p1}u+K_{i1}\frac{1}{2}u^2\right)+BB_1\delta_{r_1}+\right.$$
$$\left.CC_1\delta_{s_1}+DD_1K_{prop}+EE_1\delta_{s_2}+GG_1\delta_{r_2}\right|\eta_1,$$
$$K_8=\left|aa_2u+bb_2v+cc_2w+dd_2p+ee_2q+gg_2r+AA_2X_{prop}+BB_2\left(K_{p2}v+K_{i2}\frac{1}{2}v^2\right)+\right.$$
$$\left.CC_2\delta_{s_1}+DD_2K_{prop}+EE_2\delta_{s_2}+GG_2\delta_{r_2}\right|\eta_2,$$
$$K_9=|aa_3u+bb_3v+cc_3w+dd_3p+ee_3q+gg_3r+AA_3X_{prop}+BB_3\delta_{r_1}+$$
$$\left.CC_3\left(K_{p3}w+K_{i3}\frac{1}{2}w^2\right)+DD_3K_{prop}+EE_3\delta_{s_2}+GG_3\delta_{r_2}\right|\eta_3,$$

$$K_{10}=|aa_4u+bb_4v+cc_4w+dd_4p+ee_4q+gg_4r+AA_4X_{prop}+BB_4\delta_{r_1}+CC_4\delta_{s_1}+$$
$$\left.DD_4\left(K_{p4}p+K_{i4}\frac{1}{2}p^2\right)+EE_4\delta_{s_2}+GG_4\delta_{r_2}\right|\eta_4,$$
$$K_{11}=|aa_5u+bb_5v+cc_5w+dd_5p+ee_5q+gg_5r|\,\eta_5,$$
$$K_{12}=|aa_6u+bb_6v+cc_6w+dd_6p+ee_6q+gg_6r+AA_6X_{prop}+BB_6\delta_{r_1}+CC_6\delta_{s_1}+$$
$$\left.DD_6K_{prop}+EE_6\delta_{s_2}+GG_6\left(K_{p6}r+K_{i6}\frac{1}{2}r^2\right)\right|\eta_6,$$

where $\eta_1=\frac{1}{1-AA_1K_{d1}}$, $\eta_2=\frac{1}{1-BB_2K_{d2}}$, $\eta_3=\frac{1}{1-CC_3K_{d3}}$, $\eta_4=\frac{1}{1-DD_4K_{d4}}$, $\eta_5=\frac{1}{1-EE_5K_{d5}}$ and $\eta_6=\frac{1}{1-GG_6K_{d6}}$. Furthermore, $AA_1,K_{d1},AA_2,K_{d2},AA_3,K_{d3},AA_4,K_{d4},AA_5,K_{d5},AA_6,K_{d6}>1$. It follows that $1-AA_1K_{d1}<0$, $1-BB_2K_{d2}<0$, $1-CC_3K_{d3}<0$, $1-DD_4K_{d4}<0$, $1-EE_5K_{d5}<0$ and $1-GG_6K_{d6}<0$. Then we obtain that $\dot{V}(u,v,w,p,q,r)\le 0$. According to the above requirements, the function $V(u,v,w,p,q,r)=\frac{1}{2}u^2+\frac{1}{2}v^2+\frac{1}{2}w^2+\frac{1}{2}p^2+\frac{1}{2}q^2+\frac{1}{2}r^2$ is the Lyapunov fuction and the system is asymptotically stable.

If $V(x)\to\infty$ when $x\to\infty$, then the Lyapunov function is globally asymptotically stable. The above Lyapunov function is $V(u,v,w,p,q,r)=\frac{1}{2}u^2+\frac{1}{2}v^2+\frac{1}{2}w^2+\frac{1}{2}p^2+\frac{1}{2}q^2+\frac{1}{2}r^2$. It will be proven that $V(u,v,w,p,q,r)\to\infty$ when $u\to\infty$, $v\to\infty$, $w\to\infty$, $p\to\infty$, $q\to\infty$ and $r\to\infty$. Since $V(u,v,w,p,q,r)=\frac{1}{2}u^2+$

$\frac{1}{2}v^2 + \frac{1}{2}w^2 + \frac{1}{2}p^2 + \frac{1}{2}q^2 + \frac{1}{2}r^2$ is a quadratic function, if $u \to \infty$, $v \to \infty$, $w \to \infty$, $p \to \infty$, $q \to \infty$ and $r \to \infty$, then $V(u, v, w, p, q, r) \to \infty$. Thus, the Lyapunov function $V(u, v, w, p, q, r) = \frac{1}{2}u^2 + \frac{1}{2}v^2 + \frac{1}{2}w^2 + \frac{1}{2}p^2 + \frac{1}{2}q^2 + \frac{1}{2}r^2$ is asymptotically stable. In conclusion, the stability analysis of the SMC and SPID control systems has the stability property of being globally asymptotically stable.

9 Conclusions

Based on the simulation analysis of the SMC and SPID methods, it can be concluded that both methods have good stability for the ROV linear model with an error of about 0.09% - 4.5%. In terms of the delay time, rise time, peak time, maximum peak, and settling time, both methods have similarities. As regards the stability ratio for each motion performed, the SPID method is more stable for the surge, sway, and pitch motion, while the SMC method is more stable for the heave, roll and yaw motion.

Acknowledgement

High appreciation to the Kemdikbudristek for the very fund support for the research conducted in the year of 2023 with contract number 183/E5/PG.02.00.PL/2023, 074/SP2H/PT/LL7/2023 and 11/KP/LPPM/ITATS/2023.

References

[1] S. Subchan, T. Herlambang and H. Nurhadi. UNUSAITS AUV Navigation and Guidance System with Nonlinear Modeling Motion Using Ensemble Kalman Filter. In: *Proc. International Conference on Advanced Mechatronics, Intelligent Manufacture, and Industrial Automation (ICAMIMIA)* Malang, Indonesia, 2019.

[2] F. Chiu, J. Guo, C. Huang and W. Tsai. Application of the Sliding Mode Fuzzy Controller to the Guidance and Control of An Autonomous Underwater Vehicle. In: *Proc. International Symposium on Underwater Technology (Cat. No. 00EX418)*, 2000. 181–186.

[3] W. Naeem. Model Predictive Control of An Autonomous Underwater Vehicle. In: *Proc. UKACC Conference on Control*, 2002. 19–23.

[4] K. Kim and T. Ura. 3-Dimensional Trajectory Tracking Control of An AUV "R-One" Robot Considering Current Interaction. In: *Proc. The Twelfth International Offshore and Polar Engineering Conference*, 2002.

[5] F. Repoulias and E. Papadopoulos. Trajectory Planning and Tracking Control of Underactuated AUVs. In: *Proc. The IEEE International Conference on Robotics and Automation*, 2005. 1610—1615.

[6] L. Lapierre and D. Soetanto. Nonlinear Path-Following Control of An AUV. *Ocean Engineering* **34** (11-12) (2007) 1734–1744.

[7] H. Akçakaya, H. A. Yildiz, G. Sağlam and F. Gürleyen. Sliding Mode Control of Autonomous Underwater Vehicle. In: *Proc. International Conference on Electrical and Electronics Engineering-ELECO*, 2009. II–332.

[8] F. Rezazadegan, K. Shojaee and A. Chatraei. Design of An Adaptive Nonlinear Controller for An Autonomous Underwater Vehicle. *Int. J. Adv. Electr. Electron. Eng.* **2** (2013) 1–8.

[9] K. Oktafianto, T. Herlambang, Mardlijah and H. Nurhadi. Design of Autonomous Underwater Vehicle Motion Control Using Sliding Mode Control Method. In: *Proc. International Conference on Advanced Mechatronics, Intelligent Manufacture, and Industrial Automation (ICAMIMIA)* Surabaya, Indonesia, 2015, 162–166.

[10] T. Herlambang, S. Subchan and H. Nurhadi. Design of Motion Control Using Proportional Integral Derivative for UNUSAITS AUV. *International Review of Mechanical Engineering IREME Journal* **12** (11) (2018) 928–938.

[11] H. Nurhadi, T. Herlambang and D. Adzkiya. Design of Sliding Mode Control for Surge, Heave and Pitch Motion Control of UNUSAITS AUV. In: *Proc. International Conference on Mechanical Engineering* Indonesia, 2019.

[12] T. Herlambang, S. Subchan, H. Nurhadi and D. Adzkiya. Motion Control Design of UNUSAITS AUV Using Sliding PID. *Nonlinear Dynamics and Systems Theory* **20** (1) (2020) 51–60.

[13] F. A. Susanto, M. Y. Anshori, D. Rahmalia, K. Oktafianto, D. Adzkiya, P. Katias and T. Herlambang. Estimation of Closed Hotels and Restaurants in Jakarta as Impact of Corona Virus Disease (Covid-19) Spread Using Backpropagation Neural Network. *Nonlinear Dynamics and Systems Theory* **22** (4) (2022) 457–467.

[14] C. Yang. Modular Modeling and Control for Autonomous Underwater Vehicle (AUV). *Master's thesis, National University of Singapore* Singapore, 2007.

[15] T. Fossen. A Nonlinear Unified State-Space Model for Ship Maneuvering and Control in A Seaway. *International Journal of Bifurcation and Chaos* **15** (9) (2005) 2717—2746.

[16] W. Nie and S. Feng. Planar Path-Following Tracking Control for An Autonomous Underwater Vehicle in the Horizontal Plane. *Optik* **127** (24) (2016) 11607—11616.